

Naphtho[1,2-*b*:5,6-*b'*]dithiophene Based Two-Dimensional Conjugated Polymers for Highly Efficient Thick-Film Inverted Polymer Solar Cells

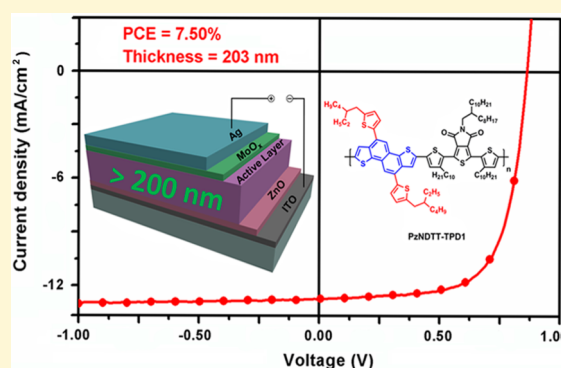
Xiangwei Zhu,^{†,‡} Jin Fang,[†] Kun Lu,^{*,†} Jianqi Zhang,[†] Lingyun Zhu,[†] Yifan Zhao,[†] Zhigang Shuai,[‡] and Zhixiang Wei^{*,†}

[†]National Center for Nanoscience and Technology, Beijing 100190, China

[‡]Department of Chemistry, Tsinghua University, Beijing 100084, China

S Supporting Information

ABSTRACT: Two-dimensional conjugated zigzag naphthodithiophene was used for construction of novel polymer photovoltaic materials. Two novel copolymers based on zigzag naphthodithiophene and alkylthieno[3,4-*c*]pyrrole-4,6-dione inserted with different alkyl substituted thiophene as bridges have been designed and synthesized (PzNDTT-TPD1 and PzNDTT-TPD2, respectively). The best power conversion efficiency of a PzNDTT-TPD1-based device reaches 7.50% at an active layer thickness of 203 nm and the device performances of PzNDTT-TPD1-based polymer solar cells are all above 6.4% with active layer thickness variations from 141 to 244 nm, suggesting that it is very suitable for the fabrication of high performance, large area solution-processed polymer solar cells.



INTRODUCTION

Over the past decade, encouraging progress has been made in the field of bulk-heterojunction (BHJ) polymer solar cells (PSCs). Power conversion efficiency (PCE) of PSCs has increased from less than 1%¹ to 10.6%² by the rational design of polymer molecules,³ the varied modification of the interface layer,⁴ the constant innovation of device structure,⁵ and so on. Even so, there exist several requirements along the road of the commercial application of PSCs, including better film-formation capability, higher efficiency, and better stability. The most prominent one is the one that indicates that optimum film forming conditions for high efficient polymers should satisfy the large area printing technology required by potential industrial production. Therefore, it is especially important for the high efficient photovoltaic materials that the device performance should be relatively independent of the film thickness of the active layers, and good performance could be obtained by using their thick-films. To date, construction of a donor-acceptor (D-A) copolymer is an effective strategy for obtaining high efficient polymer material for PSCs.⁶ However, compared with poly(3-hexylthiophene), the device performance based on most of the D-A polymers is highly dependent on active layer's film thickness. The performance of most of the D-A polymer devices normally decreases obviously as the film gets thicker than 100 nm. Only a few of them could achieve a PCE higher than 6% when the film thickness is larger than 200 nm.⁷

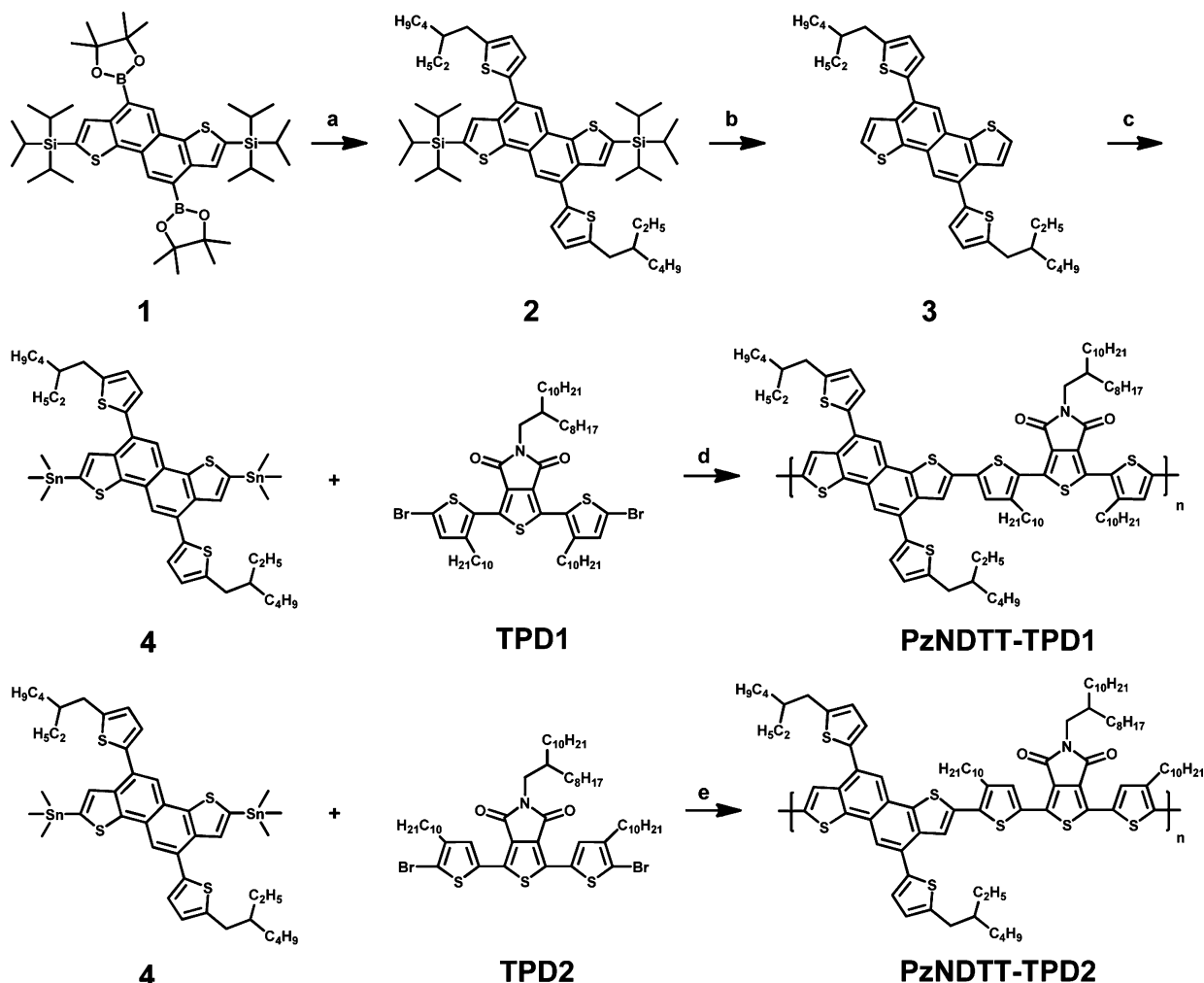
To obtain a material with good performance by using thick-films, excellent charge transport property is expected. Benzo-

[1,2-*b*:4,5-*b'*]dithiophene (BDT) is a representative building block for high mobility polymer semiconductors since it has a large planar conjugated structure and easily forms π - π stacking, which could improve charge carrier mobility.⁸ In numerous D-A copolymers, BDT-based polymers account for a substantial percentage of excellent organic photovoltaic materials whose PCEs exceed 8%.⁹ To further improve the performance of BDT based copolymers, vertical and horizontal expanding of their π -conjugated regions are carried out. Along the vertical axis, a two-dimensional (2-D) conjugated concept is applied to the BDT system, and a high PCE copolymer based on a BDT unit with two thienyl conjugated side chains (BDTT) is synthesized.¹⁰ It has been proved that 2-D conjugated polymers could exhibit red-shifted absorption spectra, lower highest occupied molecular orbital (HOMO) and lowest unoccupied molecular orbital (LUMO) energy levels, higher hole mobility, and greatly improved photovoltaic properties,¹¹ and a PCE of 8.4% was obtained as the film got thicker than 200 nm.¹² Along the horizontal axis, BDT could be extended to a tetracyclic naphthodithiophene (NDT). Just as many polycyclic aromatic hydrocarbons do, NDTs have isomeric structures including linear and zigzag shapes.¹³ Linear naphtho[2,3-*b*:6,7-*b'*]dithiophene (INDT) was preferentially introduced to the organic photovoltaic¹⁴ than zigzag naphtho[1,2-*b*:5,6-*b'*]dithiophene (zNDT).¹⁵ However, the zNDT unit is more

Received: July 25, 2014

Revised: November 28, 2014

Published: November 30, 2014

Scheme 1. Synthetic routes of PzNDTT-TPD1 and PzNDTT-TPD2^a

^aReagents and conditions: (a) 2-bromo-5-(2-ethylhexyl)thiophene, Pd(PPh₃)₄, K₃(PO₄), H₂O, THF, reflux, 24 h; (b) tetrabutylammonium fluoride, THF, room temperature, 12 h; (c) *n*-butyllithium, THF, 0 °C, 2 h, then trimethyltin chloride, room temperature, 12 h; (d) Pd₂(dba)₃, P(o-tol)₃, chlorobenzene, 130 °C, 30 h; (e) Pd₂(dba)₃, P(o-tol)₃, chlorobenzene, 130 °C, 48 h.

suitable for the construction of highly efficient D–A copolymers,¹⁶ which is probably due to its lower HOMO energy level, higher hole mobility, and higher space utilization of zigzag chemical structure than BDT and INDT.^{13a,17} Various conjugated polymers based on the zNDT unit were synthesized for high performance organic field-effect transistors (OFETs),¹⁸ and one of the zNDT-based copolymers has achieved PCE up to 8.2% even when the film thickness is larger than 200 nm.¹⁹ Integrating vertical and horizontal expanding strategy of π -conjugated region, 2-D conjugated zNDT, attaching two thienyl conjugated side chains on the zNDT core (zNDTT), might be an excellent potential candidate unit for the design and construction of highly efficient thick-film devices, for such a structure may be able to expand the conjugating surface, enhance intermolecular π – π interactions and facilitate the charge transport.

In this work, two novel copolymers based on zNDTT and alkylthieno[3,4-*c*]pyrrole-4,6-dione (TPD) inserted with different alkyl substituted thiophene as bridges have been designed and synthesized (as shown in Scheme 1). Both two polymers were obtained by a conventional polymerization method and had high solubility in many common organic solvents, which

ensure the simple solution-processed fabrication of PSC devices. As expected, the low-lying HOMO energy level and high hole mobility can be obtained by introducing the extended 2-D conjugated zNDTT unit into polymer backbones. Impressively, the device performances of PzNDTT-TPD1-based inverted PSCs are all above 6.4% with active layer thickness varying from 141 to 244 nm, indicating that the polymer is relatively not sensitive to film thickness, which is a very important characteristic to meet industrial production requirements. The best PCE reaches 7.50% at an active layer thickness of 203 nm, which gets it on to the list of only a few highly efficient polymers with film thickness more than 200 nm. Such a compatibility of high efficiency and thick active layers shows a potential application of zNDTT-based polymers in fabricating high performance, large area solution-processed PSCs.

RESULTS AND DISCUSSION

The synthetic routes of the two polymers are shown in Scheme 1. The copolymers of PzNDTT-TPD1 and PzNDTT-TPD2 were synthesized by Stille-coupling reaction using chlorobenzene as solvent and a catalyst system based on Pd₂(dba)₃ as

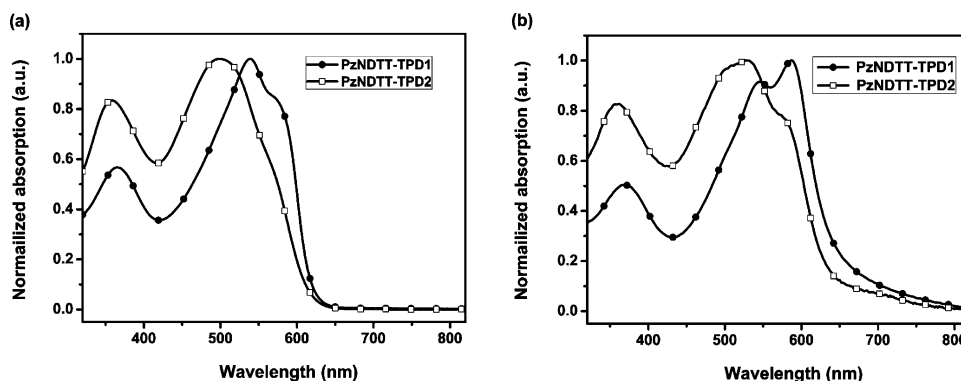


Figure 1. UV-vis absorption spectra of PzNDTT-TPD1 and PzNDTT-TPD2 in 1×10^{-5} M chlorobenzene solutions (a) and films (b).

source of palladium and P(o-tol)₃ as ligand.²⁰ Monomer 1 was prepared by the method reported in the previous literature,²¹ and the detailed synthesis procedures are described in Supporting Information (Scheme S1).

The optical properties of the two polymers were investigated by UV-vis absorption spectra both in chlorobenzene solution and thin films (Figure 1). The detailed data are also summarized in Table 1. PzNDTT-TPD1 shows an obvious

Table 1. Optical Properties and Electrochemical of Polymers

polymer	λ_{\max} [nm] solution	λ_{\max} [nm] Film	E_g^{opt} [eV]	E_g^{ec} [eV]	E_{HOMO} [eV]	E_{LUMO} [eV]
PzNDTT-TPD1	539	588	1.94	2.03	-5.55	-3.52
PzNDTT-TPD2	499	528	1.98	2.10	-5.58	-3.48

shoulder peak at ca. 570 nm in the dilute solution state (1×10^{-5} M), which can be assigned to the stronger intermolecular interactions even in dilute solution. However, the shoulder peak became weak gradually as the solution temperature increased and disappeared finally at ca. 100 °C (see Supporting Information, Figure S1), implying that PzNDTT-TPD1 chains are fully dissolved by heating. Therefore, high-temperature gel permeation chromatography (GPC) was performed on PzNDTT-TPD1 using 1,2,4-trichlorobenzene as the eluent at 140 °C (see Supporting Information, Figure S2) to validate its accurate molecular weight ($M_n = 24.9$ kDa and $M_w = 56.8$ kDa). With the formation of the film, a remarkable enhanced intensity peak at 588 nm is observed for PzNDTT-TPD1, which is an indication of an increased degree of polymer aggregation and backbone planarization compared to the solution state.²² PzNDTT-TPD2 did not show the shoulder peak in the dilute solution state, but it appeared in the film state demonstrating enhanced intermolecular interactions. From the film absorption edge of PzNDTT-TPD1, the optical band gap can be calculated as 1.94 eV, which is smaller than that of PzNDTT-TPD2 (1.98 eV). The smaller band gap of PzNDTT-TPD1 may be related to its better molecular stacking as will be discussed in the following section. Moreover, the red-shift and strong shoulder of PzNDTT-TPD1 may also be related to its higher molecule weight since the band gap decreases with the increase in molecular weight because of a longer conjugation length,²³ and molecular weight also has an influence on the vibronic structures of the peaks.²⁴ Significant influence of the alkyl chain positions was also reported on the BDT-based copolymers by Leclerc et al.²⁵

The energy levels of two polymers were determined by cyclic voltammetry (CV) measurements in thin films (see Supporting Information, Figure S3). The detailed data are also summarized in Table 1. Both the HOMO levels of the two polymers were very deep (-5.55 eV for PzNDTT-TPD1 and -5.58 eV for PzNDTT-TPD2) due to the weaker electron-donating capability of the zNDT unit. These very deep HOMO locations are a benefit for obtaining high open circuit voltage (V_{oc}) values in PSCs because the V_{oc} is mainly proportional to the energy level difference between the HOMO of the polymer donor and the LUMO of the fullerene derivative acceptor.²⁶

In order to characterize and compare the photovoltaic properties of the two polymers, PSCs were fabricated with an inverted structure of ITO/ZnO/polymer/PC₇₁BM(w/w)/MoO_x/Ag. The inverted structure was chosen here mainly due to the high stability of this kind of device toward to future applications.²⁷ Different conditions such as D/A ratios (w/w), additive ratios (v/v), and active layer thicknesses were systematically investigated to obtain the optimal device performance (see Supporting Information, Tables S1, S2, and S3). In addition, since the two polymers showed the best solubility in chloroform at low temperature, all of the films were spin-coated from the chloroform solution. First, different D/A weight ratios were tried, and the optimal ratio for both polymer-based devices was 1:1 (Table S1, Supporting Information). Then, different doses of additive, 1,8-diiodooctane (DIO), were added to the blend solution which was expected to tune the film morphology and device performance. The PCE of PzNDTT-TPD1 doubled to 5.48% by adding a very small amount of DIO (0.75%, v/v), while that of PzNDTT-TPD2 based PSC rose from 1.88% to 3.54% with 3% DIO (v/v). The results suggest that the increase of PCE arises from the addition of DIO tuning better morphology, which can be confirmed by the following atomic force microscopy (AFM) analysis. More interestingly, the PCE of PzNDTT-TPD1 could keep above 5% with only minor variations, when DIO amounts ranged from 0.5 to 5% (v/v) (Table S2, Supporting Information). One possible explanation is that the difference in the morphology of the blend films prepared with various doses of DIO is very little (see Figure S4 in Supporting Information). The similar phenomenon was also observed by Tao et al., who also used chloroform and DIO as solvent, and the changes in morphology and device performance were quite small even when DIO content increased from 1% to 6%.²⁸

Finally, the dependence of the device performance on the active layer thickness was further investigated. Generally, most

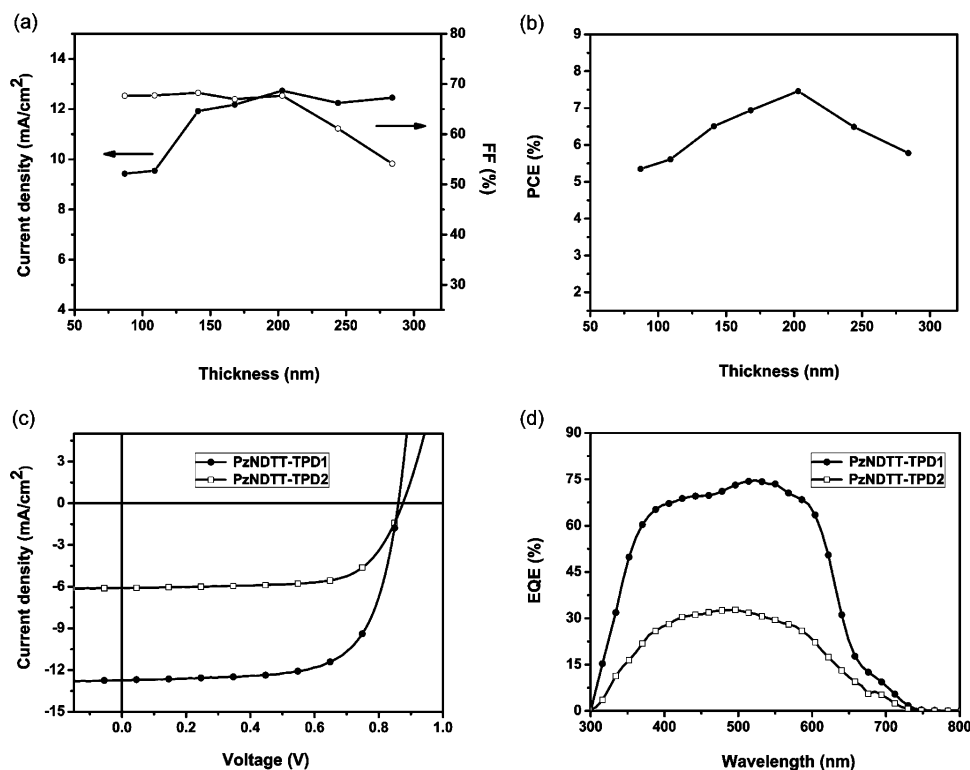


Figure 2. Plot of trends of J_{sc} /FF (a) and PCEs (b) with the active layer thickness for PzNDTT-TPD1-based inverted solar cells; the best J - V curves (c) and EQE curves (d) of inverted solar cells based on PzNDTT-TPD1/PC₇₁BM and PzNDTT-TPD2/PC₇₁BM prepared under the optimal conditions.

Table 2. Optimized Device Performance Data for PzNDTT-TPD1/PC₇₁BM as the Thickness of Active Layer Increased and the Best Data for PzNDTT-TPD2/PC₇₁BM under the Illumination of AM 1.5 G, 100 mW/cm^{2a}

polymer	V_{oc} [V]	J_{sc} [mA/cm ²]	FF	PCE [%]	thickness [nm]
PzNDTT-TPD1 ^b	0.85 (0.84 ± 0.01)	9.56 (9.35 ± 0.21)	0.68 (0.67 ± 0.01)	5.48 (5.34 ± 0.14)	87 ± 5
	0.84 (0.84 ± 0.01)	9.54 (9.50 ± 0.09)	0.70 (0.69 ± 0.01)	5.61 (5.56 ± 0.05)	109 ± 9
	0.85 (0.84 ± 0.01)	11.92 (11.02 ± 0.90)	0.66 (0.67 ± 0.03)	6.76 (6.48 ± 0.28)	141 ± 6
	0.86 (0.85 ± 0.01)	12.15 (12.28 ± 0.30)	0.68 (0.66 ± 0.02)	7.04 (6.90 ± 0.14)	168 ± 7
	0.86 (0.86 ± 0.01)	12.73 (12.52 ± 0.36)	0.68 (0.68 ± 0.02)	7.50 (7.40 ± 0.10)	203 ± 5
	0.85 (0.84 ± 0.01)	12.24 (12.35 ± 0.11)	0.62 (0.61 ± 0.01)	6.49 (6.43 ± 0.06)	244 ± 8
	0.85 (0.84 ± 0.01)	12.45 (12.59 ± 0.14)	0.55 (0.54 ± 0.02)	5.80 (5.73 ± 0.13)	284 ± 4
PzNDTT-TPD2 ^c	0.88 (0.88 ± 0.01)	6.09 (6.06 ± 0.03)	0.69 (0.67 ± 0.02)	3.68 (3.46 ± 0.22)	84 ± 6

^aDevice average values are based on more than 10 devices. The average values and variances are given in parentheses. ^bThe D/A ratio (w/w) of PzNDTT-TPD1/PC₇₁BM is 1:1; devices were prepared by adding 0.75% (v/v) DIO to the blend solution. ^cThe D/A ratio (w/w) of PzNDTT-TPD2/PC₇₁BM is 1:1; devices were prepared by adding 3% (v/v) DIO to the blend solution.

organic solar cells offer optimized PCEs when employed around 100 nm thick active layers.²⁹ Although the absorption can be enhanced by increasing the active layer thickness, an increased absorption does not result in a higher PCE when increasing the thickness beyond 100 nm since the increase in current density (J_{sc}) would be offset by the decrease in fill factor (FF). It has been pointed out that this decrease in FF originates from the enhanced charge recombination because of an increase in carrier drift length. One way to overcome this limitation is enhancing the charge carrier transport ability of the donor material.³⁰ For PzNDTT-TPD1, it is with a higher mobility after blending with PC₇₁BM (see the following section) that the J_{sc} increased continuously and the FF maintained simultaneously as the active layer thickness increased to about 200 nm (Figure 2a). Consequently, the highest PCE (7.50%) is observed at an active layer thickness of 203 nm (Figure 2b). As shown in Table 2, the average device

PCE remains above 6.4% when the film thickness ranges from 141 to 244 nm. These thick active layers with high efficiency are undoubtedly of great value for fabricating large area solution-processed PSCs. In contrast, as shown in Table S3 in Supporting Information, the performance of the PzNDTT-TPD2-based device decreased with the increase of active layer thickness. The best current–voltage (J - V) and external quantum efficiency (EQE) curves for the two polymers devices are shown in Figure 2c and d. From these charts, we observed that the wide gap of PCEs between PzNDTT-TPD1 and PzNDTT-TPD2 mainly originated from the significant difference of J_{sc} . The J_{sc} value is always determined by the hole mobility, molecular packing, and film morphology besides material absorption.³¹ Therefore, the difference of the two polymer's J_{sc} should be induced by integrating the impact of the above facts.

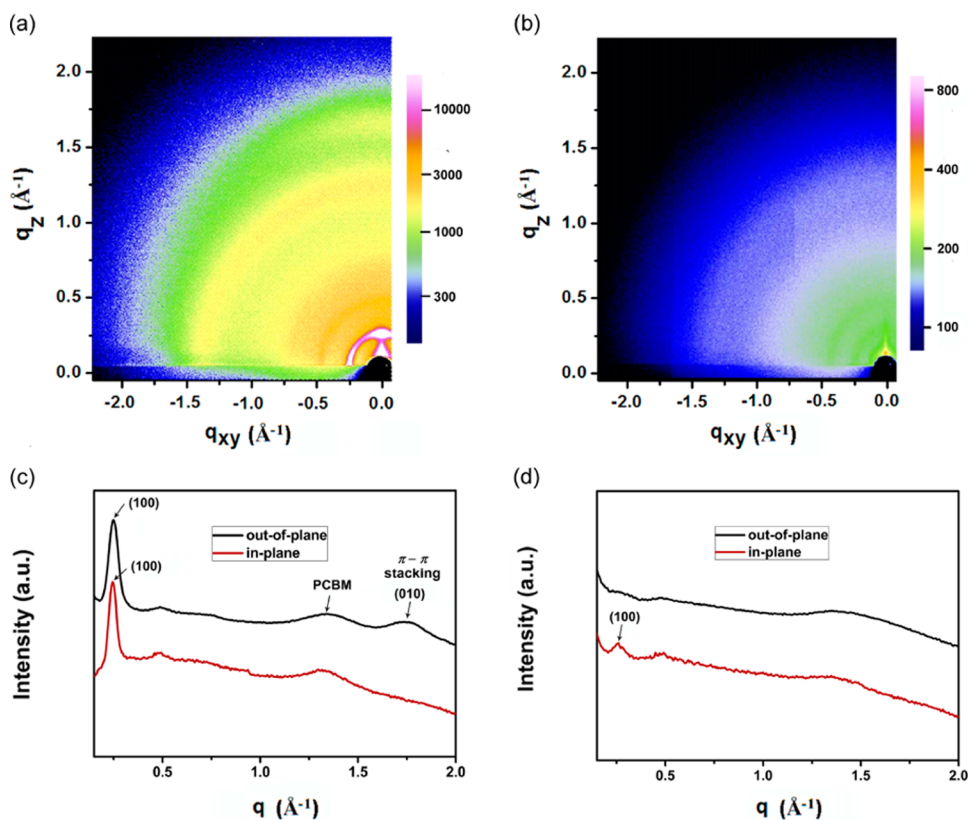


Figure 3. GIWAXS data for BHJ blend polymer films. Two-dimensional GIWAXS image of PzNDTT-TPD1/PC₇₁BM blend film with 0.75% DIO as the processing additive (a); two-dimensional GIWAXS image of PzNDTT-TPD2/PC₇₁BM blend film with 3% DIO as the processing additive (b); out-of-plane and in-plane patterns of two-dimensional GIWAXS of the PzNDTT-TPD1/PC₇₁BM blend film (c) and PzNDTT-TPD2/PC₇₁BM blend film (d).

The mobilities of the neat and blend polymer films were then tested by space-charge-limited current (SCLC) measurements (see Supporting Information, Figure S5 for the J - V characteristics). For the neat polymer, the hole mobility of PzNDTT-TPD1 ($9.1 \times 10^{-4} \text{ cm}^2 \text{ V}^{-1} \text{ s}^{-1}$) was slightly better than that of PzNDTT-TPD2 ($5.6 \times 10^{-4} \text{ cm}^2 \text{ V}^{-1} \text{ s}^{-1}$). After blending with PC₇₁BM, the gap of the mobility between the two blend films became wider. The hole mobility of the PzNDTT-TPD1/PC₇₁BM blend film rose to $1.1 \times 10^{-3} \text{ cm}^2 \text{ V}^{-1} \text{ s}^{-1}$ compared with that of the PzNDTT-TPD1 film. However, blending the other polymer with PC₇₁BM resulted in a negative consequence, and the hole mobility dropped to $3.1 \times 10^{-4} \text{ cm}^2 \text{ V}^{-1} \text{ s}^{-1}$. The hole mobilities showed differences probably because the molecular stacking mode of the two polymers have been affected by PC₇₁BM. To investigate the charge carrier transport properties of the two polymers in the lateral direction, organic field-effect transistor (OFET) devices were fabricated. Both PzNDTT-TPD1 and PzNDTT-TPD2 exhibit typical p -type organic semiconductor characteristics (see Supporting Information, Figure S6 for the output and transfer curves of two polymers). The influence of thermal treatments on performance of OFETs was also studied (see Supporting Information, Table S4). For PzNDTT-TPD1, it seems that thermal annealing had negative impact on its OFET performance since it could obtain the best OFET performance ($3.8 \times 10^{-3} \text{ cm}^2 \text{ V}^{-1} \text{ s}^{-1}$) without annealing. However, the hole mobility of PzNDTT-TPD2 could maintain about $1.2 \times 10^{-3} \text{ cm}^2 \text{ V}^{-1} \text{ s}^{-1}$ after thermal annealing at different temperatures, which is slightly higher than that obtained without thermal

annealing. In other words, the available data of SCLC and OFETs suggest that the hole mobility of PzNDTT-TPD1 was obviously higher than that of PzNDTT-TPD2. Higher hole mobility implies that the holes will be collected more quickly and that the exciton recombination probability will be reduced,³² which can partially explain the increase of J_{sc} values of PzNDTT-TPD1 devices.

To gain a deeper insight into the crystallinity and molecular stacking mode of the two polymers in the active layers, grazing-incidence wide-angle X-ray scattering (GIWAXS) analysis of the polymer/PC₇₁BM blend films with DIO additive on the ZnO-modified Si substrate was operated (Figure 3). The amorphous halo is centered at a value of q_z of 1.26 \AA^{-1} corresponding to the PC₇₁BM aggregates in the blend films.³³ The PzNDTT-TPD1/PC₇₁BM blend film shows a conspicuous diffraction (010) peak in the out-of-plane direction ($q_z \approx 1.73 \text{ \AA}^{-1}$) and a distinct (100) peak ($q_{xy} \approx 0.24 \text{ \AA}^{-1}$) in the in-plane direction, indicating the existence of a face-on orientation for PzNDTT-TPD1. The corresponding π - π stacking distance for the PzNDTT-TPD1 is ca. 3.63 \AA . Such a molecular stacking mode and shorter π - π stacking distance seem much more attractive in the PSCs.^{3d} Besides, a strong (100) peak also appears in the out-of-plane direction ($q_z \approx 0.25 \text{ \AA}^{-1}$), which might result from the interdigitation packing structure of PzNDTT-TPD1. In contrast, for the PzNDTT-TPD2/PC₇₁BM blend film, no obvious diffraction peak corresponding to π - π stacking was observed in the out-of-plane patterns, and only a very weak in-plane signal at a value of q_z of 0.26 \AA^{-1} arose, suggesting that the blend film tends to be more amorphous and

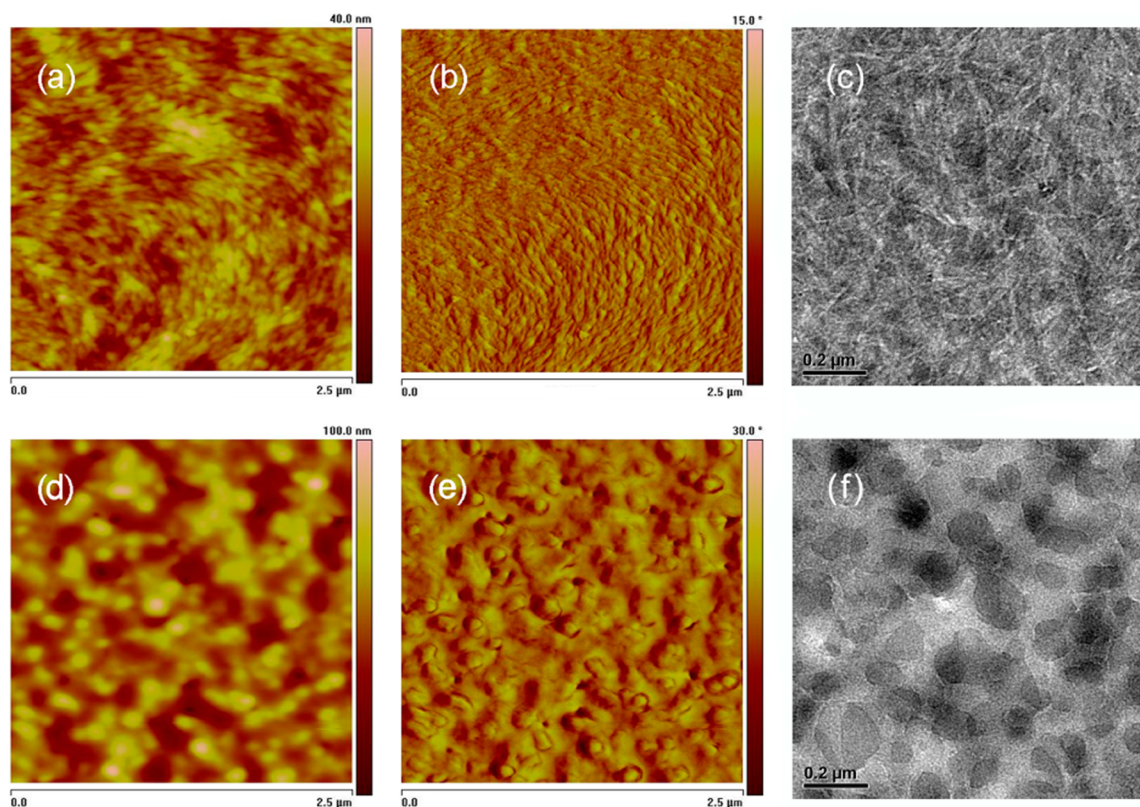


Figure 4. Tapping mode AFM topography, phase, and TEM images of PzNDTT-TPD1/PC₇₁BM = 1:1 (w/w) processed by chloroform with 0.75% DIO additive at the optimal thickness (203 nm) (a–c); PzNDTT-TPD2/PC₇₁BM = 1:1 (w/w) processed by chloroform with 3% DIO additive at the optimal thickness (84 nm) (d–f). The size of the AFM image is 2.5 μm × 2.5 μm. The bar in the TEM image represents 200 nm.

that few ordered structures formed. Compared with PzNDTT-TPD2, more ordered structure and superior crystallization capability in the blend film for PzNDTT-TPD1 are consistent with its higher hole mobility, which would presumably promote the significant improvement of J_{sc} .

Furthermore, atomic force microscopy (AFM) and transmission electron microscope (TEM) analyses were also carried out to validate the performance difference. AFM images reveal the presence of large domains and a high level of aggregation in the two polymers/PC₇₁BM blend films without the DIO additive (see Supporting Information, Figure S7). By adding very small amounts of DIO, the optimal blend film of PzNDTT-TPD1/PC₇₁BM exhibits much smaller domain size in the AFM image. Some widely distributed fibrillar structures are clearly observed in the whole film (Figure 4b). The TEM image (Figure 4c) also displays that polymer nanofibrils with diameters of tens of nanometers have been achieved and that PC₇₁BM can be well intermixed between them. Such an interpenetrating bicontinuous network morphology could be beneficial to exciton diffusion and charge separation.³⁴ In contrast, for the optimal blend film of PzNDTT-TPD2/PC₇₁BM, the morphology has not obviously improved with the addition of DIO. Some island aggregations also appear in the phase image (Figure 4e), and in the corresponding TEM image (Figure 4f), obvious PC₇₁BM aggregations with the feature size of hundreds of nanometers are presented. This large scale phase separation would diminish the exciton migration to the polymer/PC₇₁BM interface and influence the following charge separation and collection, resulting in lower J_{sc} and worse PCE performance.³⁵ Benefiting from the more optimized morphology, PzNDTT-TPD1 yielded a significant increase in J_{sc}

compared with PzNDTT-TPD2, leading finally to a high PCE performance.

CONCLUSIONS

In summary, two novel copolymers based on zNDTT as the donor and TPD as the acceptor with different alkyl substituted thiophene bridges, PzNDTT-TPD1 and PzNDTT-TPD2, have been synthesized. As expected, the low-lying HOMO energy level and high hole mobility can be obtained by introducing the extended 2-D conjugated zNDTT unit into polymer backbones. Encouragingly, all of the PCE values of inverted BHJ solar cells based on PzNDTT-TPD1/PC₇₁BM with active layer thickness variations from 141 to 244 nm are above 6.4%, and the highest PCE reaches 7.5% with an active layer thickness of 203 nm. The enhanced absorption derived from the increase in the active layer thickness remedies a major defect of large band gap, turning PzNDTT-TPD1 to a high efficient donor material with a normal absorption spectrum. These results suggest that 2-D conjugated zNDT (zNDTT) might be a very promising candidate unit for the design and construction of novel highly efficient donor materials with thick active layers.

ASSOCIATED CONTENT

Supporting Information

Experimental section, UV absorption spectra, high-temperature GPC data, CV curves, J – V characteristics of SCLC, output, and transfer characteristics of OFET, AFM images, and other device data. This material is available free of charge via the Internet at <http://pubs.acs.org>.

■ AUTHOR INFORMATION

Corresponding Authors

*(K.L.) E-mail: lvk@nanocr.cn.

*(Z.W.) E-mail: weizx@nanocr.cn.

Notes

The authors declare no competing financial interest.

■ ACKNOWLEDGMENTS

We acknowledge the financial support by the National Natural Science Foundation of China (Grant No. 21125420), the Ministry of Science and Technology of China (Grant No. 2011CB932300), and the Chinese Academy of Sciences.

■ REFERENCES

(1) Yu, G.; Gao, J.; Hummelen, J. C.; Wudl, F.; Heeger, A. J. *Science* **1995**, *270*, 1789–1791.

(2) You, J. B.; Dou, L. T.; Yoshimura, K.; Kato, T.; Ohya, K.; Moriarty, T.; Emery, K.; Chen, C. C.; Gao, J.; Li, G.; Yang, Y. *Nat. Commun.* **2013**, *4*, 1446.

(3) (a) Mühlbacher, D.; Scharber, M.; Morana, M.; Zhu, Z.; Waller, D.; Gaudiana, R.; Brabec, C. *Adv. Mater.* **2006**, *18*, 2884–2889. (b) Blouin, N.; Michaud, A.; Leclerc, M. *Adv. Mater.* **2007**, *19*, 2295–2300. (c) Liang, Y.; Xu, Z.; Xia, J.; Tsai, S.-T.; Wu, Y.; Li, G.; Ray, C.; Yu, L. *Adv. Mater.* **2010**, *22*, E135–E138. (d) Guo, X.; Zhou, N.; Lou, S. J.; Smith, J.; Tice, D. B.; Hennek, J. W.; Ortiz, R. P.; Navarrete, J. T. L.; Li, S.; Strzalka, J.; Chen, L. X.; Chang, R. P. H.; Facchetti, A.; Marks, T. J. *Nat. Photonics* **2013**, *7*, 825–833. (e) Dou, L.; Chen, C.-C.; Yoshimura, K.; Ohya, K.; Chang, W.-H.; Gao, J.; Liu, Y.; Richard, E.; Yang, Y. *Macromolecules* **2013**, *46*, 3384–3390.

(4) (a) Brabec, C. J.; Shaheen, S. E.; Winder, C.; Sariciftci, N. S.; Denk, P. *Appl. Phys. Lett.* **2002**, *80*, 1288–1290. (b) Kim, J. Y.; Kim, S. H.; Lee, H. H.; Lee, K.; Ma, W.; Gong, X.; Heeger, A. J. *Adv. Mater.* **2006**, *18*, S72–S76. (c) Sun, Y.; Takacs, C. J.; Cowan, S. R.; Seo, J. H.; Gong, X.; Roy, A.; Heeger, A. J. *Adv. Mater.* **2011**, *23*, 2226–2230. (d) He, Z.; Zhong, C.; Huang, X.; Wong, W.-Y.; Wu, H.; Chen, L.; Su, S.; Cao, Y. *Adv. Mater.* **2011**, *23*, 4636–4643. (e) Sun, Z.; Xiao, K.; Keum, J. K.; Yu, X.; Hong, K.; Browning, J.; Ivanov, I. N.; Chen, J.; Alonzo, J.; Li, D.; Sumpter, B. G.; Payzant, E. A.; Rouleau, C. M.; Geohagan, D. B. *Adv. Mater.* **2011**, *23*, 5529–5535. (f) Liu, S.; Zhang, K.; Lu, J.; Zhang, J.; Yip, H.-L.; Huang, F.; Cao, Y. *J. Am. Chem. Soc.* **2013**, *135*, 15326–15329.

(5) (a) Waldauf, C.; Morana, M.; Denk, P.; Schilinsky, P.; Coakley, K.; Choulis, S. A.; Brabec, C. J. *Appl. Phys. Lett.* **2006**, *89*, 233517–233517. (b) White, M. S.; Olson, D. C.; Shaheen, S. E.; Kopidakis, N.; Ginley, D. S. *Appl. Phys. Lett.* **2006**, *89*, 143513–143517. (c) Kim, J. Y.; Lee, K.; Coates, N. E.; Moses, D.; Nguyen, T.-Q.; Dante, M.; Heeger, A. J. *Science* **2007**, *317*, 222–225. (d) Sista, S.; Park, M.-H.; Hong, Z.; Wu, Y.; Hou, J.; Kwan, W. L.; Li, G.; Yang, Y. *Adv. Mater.* **2010**, *22*, 380–383.

(6) (a) Svensson, M.; Zhang, F. L.; Veenstra, S. C.; Verhees, W. J. H.; Hummelen, J. C.; Kroon, J. M.; Inganas, O.; Andersson, M. R. *Adv. Mater.* **2003**, *15*, 988–991. (b) Hou, J. H.; Chen, H. Y.; Zhang, S. Q.; Li, G.; Yang, Y. *J. Am. Chem. Soc.* **2008**, *130*, 16144–16145. (c) Liang, Y. Y.; Wu, Y.; Feng, D. Q.; Tsai, S. T.; Son, H. J.; Li, G.; Yu, L. P. *J. Am. Chem. Soc.* **2009**, *131*, 56–57. (d) Inganas, O.; Zhang, F.; Andersson, M. R. *Acc. Chem. Res.* **2009**, *42*, 1731–1739. (e) Chen, J.; Cao, Y. *Acc. Chem. Res.* **2009**, *42*, 1709–1718. (f) Li, Y. *Acc. Chem. Res.* **2012**, *45*, 723–733.

(7) (a) Chu, T.-Y.; Lu, J.; Beaupré, S.; Zhang, Y.; Pouliot, J.-R.; Wakim, S.; Zhou, J.; Leclerc, M.; Li, Z.; Ding, J.; Tao, Y. *J. Am. Chem. Soc.* **2011**, *133*, 4250–4253. (b) Price, S. C.; Stuart, A. C.; Yang, L.; Zhou, H.; You, W. *J. Am. Chem. Soc.* **2011**, *133*, 4625–4631. (c) Wang, M.; Hu, X.; Liu, P.; Li, W.; Gong, X.; Huang, F.; Cao, Y. *J. Am. Chem. Soc.* **2011**, *133*, 9638–9641. (d) Guo, X.; Cui, C. H.; Zhang, M. J.; Huo, L. J.; Huang, Y.; Hou, J. H.; Li, Y. *Energy Environ. Sci.* **2012**, *5*, 7943–7949. (e) Li, K.; Li, Z.; Feng, K.; Xu, X.; Wang, L.; Peng, Q. *J. Am. Chem. Soc.* **2013**, *135*, 13549–13557. (f) Li, W.; Hendriks, K. H.;

Roelofs, W. S. C.; Kim, Y.; Wienk, M. M.; Janssen, R. A. J. *Adv. Mater.* **2013**, *25*, 3182–3186. (g) Chen, Z.; Cai, P.; Chen, J.; Liu, X.; Zhang, L.; Lan, L.; Peng, J.; Ma, Y.; Cao, Y. *Adv. Mater.* **2014**, *26*, 2586–2591. (h) Gao, J.; Dou, L.; Chen, W.; Chen, C.-C.; Guo, X.; You, J.; Bob, B.; Chang, W.-H.; Strzalka, J.; Wang, C.; Li, G.; Yang, Y. *Adv. Energy Mater.* **2014**, DOI: 10.1002/aenm.201300739. (i) Hu, X.; Yi, C.; Wang, M.; Hsu, C.-H.; Liu, S.; Zhang, K.; Zhong, C.; Huang, F.; Gong, X.; Cao, Y. *Adv. Energy Mater.* **2014**, DOI: 10.1002/aenm.201400378. (j) Nguyen, T. L.; Choi, H.; Ko, S. J.; Uddin, M. A.; Walker, B.; Yum, S.; Jeong, J. E.; Yun, M. H.; Shin, T. J.; Hwang, S.; Kim, J. Y.; Woo, H. Y. *Energy Environ. Sci.* **2014**, *7*, 3040–3051. (k) Liu, Y.; Zhao, J.; Li, Z.; Mu, C.; Ma, W.; Hu, H.; Jiang, K.; Lin, H.; Ade, H.; Yan, H. *Nat. Commun.* **2014**, *5*, 5293.

(8) Hou, J. H.; Park, M. H.; Zhang, S. Q.; Yao, Y.; Chen, L. M.; Li, J. H.; Yang, Y. *Macromolecules* **2008**, *41*, 6012–6018.

(9) (a) Chen, H.-C.; Chen, Y.-H.; Liu, C.-C.; Chien, Y.-C.; Chou, S.-W.; Chou, P.-T. *Chem. Mater.* **2012**, *24*, 4766–4772. (b) Zhang, M.; Gu, Y.; Guo, X.; Liu, F.; Zhang, S.; Huo, L.; Russell, T. P.; Hou, J. *Adv. Mater.* **2013**, *25*, 4944–4949. (c) Cabanetos, C.; El Labban, A.; Bartelt, J. A.; Douglas, J. D.; Mateker, W. R.; Fréchet, J. M. J.; McGehee, M. D.; Beaujeu, P. M. *J. Am. Chem. Soc.* **2013**, *135*, 4656–4659. (d) Wang, N.; Chen, Z.; Wei, W.; Jiang, Z. *J. Am. Chem. Soc.* **2013**, *135*, 17060–17068. (e) Zhang, M.; Guo, X.; Zhang, S.; Hou, J. *Adv. Mater.* **2014**, *26*, 1118–1123.

(10) Huo, L. J.; Hou, J. H.; Zhang, S. Q.; Chen, H. Y.; Yang, Y. *Angew. Chem., Int. Ed.* **2010**, *49*, 1500–1503.

(11) Huo, L. J.; Zhang, S. Q.; Guo, X.; Xu, F.; Li, Y. F.; Hou, J. H. *Angew. Chem., Int. Ed.* **2011**, *50*, 9697–9702.

(12) Yang, T. B.; Wang, M.; Duan, C. H.; Hu, X. W.; Huang, L.; Peng, J. B.; Huang, F.; Gong, X. *Energy Environ. Sci.* **2012**, *5*, 8208–8214.

(13) (a) Shinamura, S.; Miyazaki, E.; Takimiya, K. *J. Org. Chem.* **2010**, *75*, 1228–1234. (b) Shinamura, S.; Osaka, I.; Miyazaki, E.; Nakao, A.; Yamagishi, M.; Takeya, J.; Takimiya, K. *J. Am. Chem. Soc.* **2011**, *133*, 5024–5035.

(14) Loser, S.; Bruns, C. J.; Miyauchi, H.; Ortiz, R. P.; Facchetti, A.; Stupp, S. I.; Marks, T. J. *J. Am. Chem. Soc.* **2011**, *133*, 8142–8145.

(15) Osaka, I.; Abe, T.; Shimawaki, M.; Koganezawa, T.; Takimiya, K. *ACS Macro Lett.* **2012**, *1*, 437–440.

(16) Shi, S. W.; Jiang, P.; Yu, S. Q.; Wang, L. W.; Wang, X. C.; Wang, M.; Wang, H. Q.; Li, Y. F.; Li, X. Y. *J. Mater. Chem. A* **2013**, *1*, 1540–1543.

(17) (a) Takimiya, K.; Kunugi, Y.; Konda, Y.; Niihara, N.; Otsubo, T. *J. Am. Chem. Soc.* **2004**, *126*, 5084–5085. (b) Takimiya, K.; Konda, Y.; Ebata, H.; Niihara, N.; Otsubo, T. *J. Org. Chem.* **2005**, *70*, 10569–10571.

(18) (a) Osaka, I.; Abe, T.; Shinamura, S.; Miyazaki, E.; Takimiya, K. *J. Am. Chem. Soc.* **2010**, *132*, 5000–5001. (b) Osaka, I.; Abe, T.; Shinamura, S.; Takimiya, K. *J. Am. Chem. Soc.* **2011**, *133*, 6852–6860.

(19) Osaka, I.; Kakara, T.; Takemura, N.; Koganezawa, T.; Takimiya, K. *J. Am. Chem. Soc.* **2013**, *135*, 8834–8837.

(20) Li, J.; Zhao, Y.; Tan, H. S.; Guo, Y. L.; Di, C. A.; Yu, G.; Liu, Y. Q.; Lin, M.; Lim, S. H.; Zhou, Y. H.; Su, H. B.; Ong, B. S. *Sci. Rep.* **2012**, *2*, 754.

(21) Shinamura, S.; Sugimoto, R.; Yanai, N.; Takemura, N.; Kashiki, T.; Osaka, I.; Miyazaki, E.; Takimiya, K. *Org. Lett.* **2012**, *14*, 4718–4721.

(22) Zhong, H. L.; Li, Z.; Deledalle, F.; Fregoso, E. C.; Shahid, M.; Fei, Z. P.; Nielsen, C. B.; Yaacobi-Gross, N.; Rossbauer, S.; Anthopoulos, T. D.; Durrant, J. R.; Heeney, M. *J. Am. Chem. Soc.* **2013**, *135*, 2040–2043.

(23) Kroon, R.; Lenes, M.; Hummelen, J. C.; Blom, P. W. M.; de Boer, B. *Polym. Rev.* **2008**, *48*, 531–582.

(24) Ashraf, R. S.; Schroeder, B. C.; Bronstein, H. A.; Huang, Z.; Thomas, S.; Kline, R. J.; Brabec, C. J.; Rannou, P.; Anthopoulos, T. D.; Durrant, J. R.; McCulloch, I. *Adv. Mater.* **2013**, *25*, 2029–2034.

(25) Najari, A.; Beaupré, S.; Berrouard, P.; Zou, Y. P.; Pouliot, J. R.; Lepage-Perusse, C.; Leclerc, M. *Adv. Funct. Mater.* **2011**, *21*, 718–728.

- (26) Scharber, M. C.; Mühlbacher, D.; Koppe, M.; Denk, P.; Waldauf, C.; Heeger, A. J.; Brabec, C. J. *Adv. Mater.* **2006**, *18*, 789–794.
- (27) Hau, S. K.; Yip, H.-L.; Baek, N. S.; Zou, J.; Omalley, K.; Jen, A. *K. Y. Appl. Phys. Lett.* **2008**, *92*, 253301–253303.
- (28) Zhang, Y.; Li, Z.; Wakim, S.; Alem, S.; Tsang, S.-W.; Lu, J.; Ding, J.; Tao, Y. *Org. Electron.* **2011**, *12*, 1211–1215.
- (29) Kroon, R.; Diaz de Zerio Mendaza, A.; Himmelberger, S.; Bergqvist, J.; Bäcke, O.; Faria, G. C.; Gao, F.; Obaid, A.; Zhuang, W.; Gedefaw, D.; Olsson, E.; Inganäs, O.; Salleo, A.; Müller, C.; Andersson, M. R. *J. Am. Chem. Soc.* **2014**, *136*, 11578–11581.
- (30) Lenes, M.; Koster, L. J. A.; Mihailetschi, V. D.; Blom, P. W. M. *Appl. Phys. Lett.* **2006**, *88*, 243502.
- (31) Li, G.; Zhu, R.; Yang, Y. *Nat. Photonics* **2012**, *6*, 153–161.
- (32) Loser, S.; Miyauchi, H.; Hennek, J. W.; Smith, J.; Huang, C.; Facchetti, A.; Marks, T. J. *Chem. Commun.* **2012**, *48*, 8511–8513.
- (33) Su, M.-S.; Kuo, C.-Y.; Yuan, M.-C.; Jeng, U. S.; Su, C.-J.; Wei, K.-H. *Adv. Mater.* **2011**, *23*, 3315–3319.
- (34) Halls, J. J. M.; Pichler, K.; Friend, R. H.; Moratti, S. C.; Holmes, A. B. *Appl. Phys. Lett.* **1996**, *68*, 3120–3122.
- (35) Chung, H.-S.; Lee, W.-H.; Song, C. E.; Shin, Y.; Kim, J.; Lee, S. K.; Shin, W. S.; Moon, S.-J.; Kang, I.-N. *Macromolecules* **2013**, *47*, 97–105.